THE ASTROPHYSICAL JOURNAL, 461:210–222, 1996 April 10

THE INFRARED SPECTRUM OF THE GALACTIC CENTER AND THE COMPOSITION OF INTERSTELLAR DUST

A. G. G. M. TIELENS,[1] D. H. WOODEN,[2] L. J. ALLAMANDOLA,[2] J. BREGMAN,[2] AND F. C. WITTEBORN[2]
Received 1995 July 21; accepted 1995 October 18

ABSTRACT

We have obtained 5–8 μm spectra of the Galactic center from the Kuiper Airborne Observatory at resolving powers of ≈ 50, ≈ 150, and ≈ 300. These spectra show absorption features at 5.5, 5.8, 6.1, and 6.8 μm. Together with previously observed features in the 3 μm region, these features are compared with laboratory spectra of candidate materials. The 3.0 and 6.1 μm features are due to the OH stretching and bending variations of H_2O and are well fitted by water of hydration in silicates (e.g., talc). The 3.0 μm band is equally well fitted by ice mixtures containing 30% H_2O, but such mixtures do not provide a good fit to the observed 6.1 μm band. The 3.4 and 6.8 μm features are identified with the CH stretching and deformation modes in CH_2 and CH_3 groups in saturated aliphatic hydrocarbons. The 6.1 μm band shows a short wavelength shoulder centered on 5.8 μm, attributed to carbonyl (C=O) groups in this interstellar hydrocarbon dust component. Finally, the narrow 5.5 μm feature is also attributed to carbonyl groups, but in the form of metal carbonyls [e.g., $Fe(CO)_4$].

We have derived column densities and abundances along the line of sight toward the Galactic center for the various identified dust components. This analysis shows that hydrocarbon grains contain only 0.08 of the elemental abundance of C and contribute only a relatively minor fraction (0.1) of the total dust volume. Most of the interstellar dust volume is made up of silicates (≈ 0.6). Small graphite grains, responsible for the 2200 Å bump, account for 0.07 of the total dust volume. The remaining one-quarter of the interstellar dust volume consists of a material(s) without strong IR absorption features. Likely candidates include large graphite grains, diamonds, or amorphous carbon grains, which all have weak or no IR active modes. Finally, various models for the origin of the hydrocarbon dust component of the interstellar dust are discussed. All of them face some problems in explaining the observations, in particular, the absence of the spectroscopic signature of hydrocarbon grains in sources associated with molecular clouds.

Subject headings: dust, extinction — Galaxy: center — infrared: ISM: lines and bands — ISM: abundances

1. INTRODUCTION

Despite 50 years of active research, the composition of dust in the diffuse interstellar medium (ISM) is still quite uncertain. Most researchers in this field agree that silicates and some form of carbon dominate interstellar dust. Some researchers think that the carbon is mainly in the form of graphite (Mathis, Rumpl, & Nordsieck 1977; Draine & Lee 1984). This is based on the strong 2200 Å bump in the interstellar extinction curve, which is attributed to small (≈ 200 Å) graphite grains (Gilra 1973; Draine & Lee 1984). In these grain models, it is assumed that, besides the 200 Å grains, larger (≈ 1000–2500 Å) graphite grains are also present, which then produce a large fraction of the visible extinction. The remainder of the visible and far-ultraviolet (FUV) extinction and the visible polarization are produced by silicate grains with sizes in the range 100–2500 Å (Mathis et al. 1977; Mathis 1979; Draine & Lee 1984).

In an alternative dust model, solid carbon is postulated to be mainly in the form of large organic molecules in grain mantles on silicate cores (Greenberg 1979). Some carbon is still assumed to be present in the form of graphite or amorphous carbon material in order to explain the 2200 Å bump. The bulk of the visible extinction and polarization, however, is attributed to these organic grain mantles (Greenberg & Chlewicki 1984). These complex molecular grain mantles are presumed to be formed by UV photolysis of simple molecular mixtures, accreted inside dense molecular clouds on preexisting silicate grains (Greenberg 1979). There is good observational evidence for the progenitor icy grain mantles, consisting of simple molecules such as H_2O, CH_3OH, and CO, inside dense molecular clouds (see Tielens 1989 for a review). However, direct observational evidence for complex grain mantles in the diffuse ISM is more scant.

The extinction along the line of sight toward the Galactic center is believed to be dominated by dust in the diffuse ISM. Because of the high extinction and high IR flux, the IR spectra of Galactic center sources have been a prime sampling ground for the characteristics of interstellar dust. Indeed, the presence of complex molecular grain mantles in the diffuse ISM was first surmised from the presence of a set of absorption features around 3.4 μm in the spectra of sources in the Galactic center (Willner et al. 1979; Allen & Wickramasinghe 1981; Jones, Hyland, & Allen 1983; Butchart et al. 1986). Recently, these features have also been detected in several other lines of sight (Adamson, Whittet, & Duley 1990; Sandford et al. 1991; Pendleton et al. 1994). These features are due to the symmetric and asymmetric CH stretching modes of CH_2 and CH_3 groups in saturated aliphatic hydrocarbons or related organic compounds. These absorption features are absent in sources whose extinction is dominated by newly formed circumstellar dust, and, hence, they are thought to be carried by a dust component formed in the ISM itself.

[1] MS 245-3, NASA Ames Research Center, Moffett Field, CA 94035.
[2] MS 245-6, NASA Ames Research Center, Moffett Field, CA 94035.

The identification of the 3.4 and 3.48 μm features with CH stretching modes predicts the presence of CH deformation modes around 6.8 μm. The ratio of the strength of the CH deformation to that of the stretching modes is very indicative of the class of aliphatic molecules present (Bellamy 1960; Wexler 1967). Other important absorptions which occur in the 5–8 μm region are the carbonyl (C=O) stretch and the OH and NH bending vibrations. Since this spectral region is so diagnostic for grain composition, we have obtained 5–8 μm spectra of the Galactic center. The observations and their analysis are described in §§ 2 and 3, respectively. In § 4, the absorption features in the 3–8 μm spectrum of the Galactic center are analyzed, and their carriers identified. Abundances of various interstellar dust components are derived and compared in § 5, and the origin of the hydrocarbon dust component of the interstellar dust is discussed in § 6. Finally, the results are summarized in § 7.

2. OBSERVATIONS

2.1. *Faint Object Grating Spectrometer Observations*

2.1.1. *Low-Resolution Observations*

A low-resolution (channel width 0.12 μm, $\lambda/\Delta\lambda \approx 50$), 5–8 μm spectrum of the Galactic center was obtained with the Faint Object Grating Spectrometer (FOGS), a 24 element, multiplexed grating spectrometer, on one flight (1985 May 28) of the Kuiper Airborne Observatory (KAO) from Ames. Details of the spectrometer and the observing procedure have been presented elsewhere (Witteborn & Bregman 1984). The observations were made with a 21″ aperture centered on Sgr A IRS 3 and a chopper throw of 2′. The spectrum was calibrated against α Boo.

Due to rolling of the airplane and the low elevation of Sgr A on flights originating from Ames, the telescope lost track at various times. If it lost track for longer than 20 s during 2 minute integrations, the integration was aborted and only restarted after the object had been acquired again. The Galactic center spectrum shown in the top panel of Figure 1 represents 16 minutes of integration during a 1 hr observing leg. The statistical noise, about 3×10^{-17} W cm^{-2} μm^{-1}—corresponding to a signal-to-noise ratio of about 30—is somewhat large compared with previous performances of the FOGS on the KAO. This is mainly due to the frequent loss of track. However, because all channels are observing at the same time, the shape of the spectrum is probably more accurate than the signal-to-noise level indicates. No correction has been applied to the statistical error estimates for this effect.

2.1.2. *Moderate-Resolution Observations*

The original design of the FOGS (Witteborn & Bregman 1984) has been modified to incorporate an externally rotatable grating table and an aperture and order sorter filter wheel. The grating used for these observations had 210 grooves mm^{-1} and was blazed for 4.3 μm in first order, resulting in a spectral resolution of 0.047–0.038 μm per detector ($\lambda/\Delta\lambda = 110$–210). The first detector was noisy, and its results have been deleted from the resulting spectra. A focal-plane aperture of 13.″6 was used, and the spectra were calibrated against Sirius, using the calibration procedure derived by Cohen et al. (1992). The statistical noise is about 10^{-17} W cm^{-2} μm^{-1}.

The observations of Sgr A IRS 3 in this configuration were obtained on the KAO on 1989 April 10, on one flight from Christchurch, New Zealand. The 5–8 μm spectrum shown in the middle panel of Figure 1 was constructed from four independent, partially overlapping (3–4 detectors), grating settings. Two of these were centered at about 5.8 and 7.6 μm, respectively. The other two were both centered at about 6.8 μm but shifted by half a resolution element. Wavelength calibration was achieved by obtaining spectra of an on-board blackbody through a polystyrene sample or a methane gas cell. Due to small pointing variations during the observations, the four different grating settings have small (10%) differences in absolute flux level in the region of

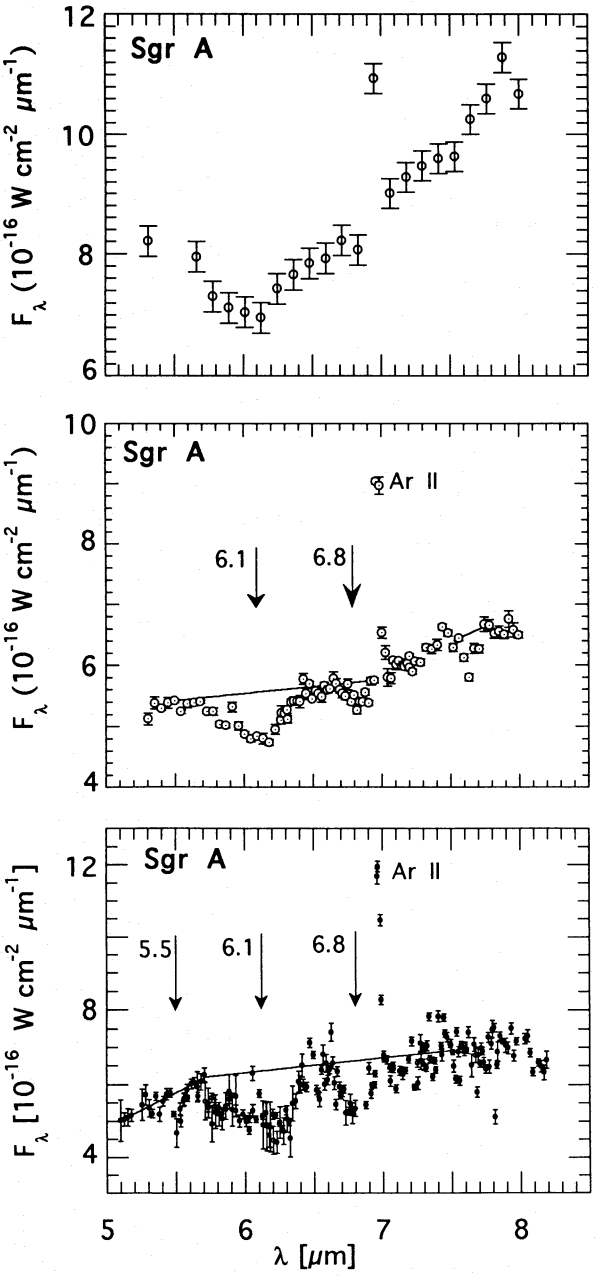

FIG. 1.—Low-resolution ($\lambda/\Delta\lambda \approx 50$) 5–8 μm spectrum of the Galactic center obtained with the FOGS (*top*). Medium-resolution ($\lambda/\Delta\lambda \approx 110$–210) 5–8 μm spectrum of the Galactic center obtained with the FOGS (*middle*). Medium-resolution ($\lambda/\Delta\lambda \approx 210$–340) 5–8 μm spectrum of the Galactic center obtained with the HIFOGS (*bottom*). Absorption features at 5.5, 6.1, and 6.8 μm and the Ar II line at 6.99 μm are indicated. The linear baselines, which have been used to derive the shape of the absorption features, are shown as solid lines.

overlap. The different settings have been joined by normalization in this overlap region.

2.2. *High-Efficiency Infrared Faint Object Grating Spectrometer Observations*

The High-Efficiency Infrared Faint Object Grating Spectrometer (HIFOGS) is a significant modification of the FOGS design that permits simultaneous coverage over a wide spectral range. It incorporates a linear array of 120 Si:Bi detectors (Witteborn et al. 1995). A grating with 148 grooves mm^{-1} was used, providing a resolving power of 210–340. A focal-plane aperture of 13″.6 was centered on Sgr A IRS 3. The wavelength was calibrated by obtaining a spectrum of an on-board blackbody through a polystyrene filter. A spectrum of the Galactic center was obtained on a flight from NASA Ames to Honolulu, Hawaii, on 1994 April 5. Two independent settings, shifted by 0.25 μm, were used to obtain Nyquist sampling. The spectra were calibrated against α Her obtained on the same flight. The absolute flux spectrum of α Her was calibrated against Sirius on another flight during this same flight series using the Kurucz model atmosphere of Sirius degraded to the HIFOGS resolution (Cohen et al. 1992, 1995). Careful examination of these settings as well as other spectra obtained on this flight series showed that about 8% of the detectors were unusable (much lower responsivity than adjacent detectors and nonlinear in response), and they have been deleted from the final spectrum. The flux of the long-wavelength setting has been shifted upward by 7%, to ensure better agreement, before interleaving the two settings (Fig. 1, *bottom panel*). The spectra were corrected for telluric absorption using ATRAN, adopting the air mass of the object and the standard and assuming 12 μm of precipitable water at airplane altitudes. The spectrum represents about 30 minutes integration per setting and has a statistical noise of about 2×10^{-17} W cm^{-2} μm^{-1}.

3. THE 5–8 μm SPECTRUM OF Sgr A

The spectra shown in Figure 1 agree very well in overall shape. They clearly show a very broad absorption feature at about 6.1 μm. A weaker and narrower feature at about 6.8 μm, hinted at in the low-resolution data, is clearly present in the moderate-resolution FOGS and HIFOGS spectra. The HIFOGS spectrum also shows a narrow absorption feature at 5.5 μm that is present as a one-channel dip in the moderate-resolution FOGS spectrum, which has lower resolution (≈100 vs. ≈200) at these wavelengths. Finally, the Ar II line at 6.99 μm is prominent in all three spectra.

3.1. *The Adopted Mid-IR Continuum*

The Galactic center is a complex region, and many distinct sources as well as an extended background contribute to its IR emission (Rieke & Low 1973; Rieke, Telesco, & Harper 1978; Becklin et al. 1978a, b; Gezari et al. 1985). Between 5 and 8 μm, the dominant *compact* source is IRS 3, which, however, contributes only about 25% at 5 μm and 10% at 8 μm to the observed flux in the low-resolution spectrum (21″ beam). Most of the observed emission in this spectrum results from the extended ridge of emission associated with the H II region, IRS 1. The moderate-resolution spectra were obtained in smaller beams (13″.6), and, relatively speaking, IRS 3 is about twice as important. Nevertheless, even in this spectrum, most of the flux, particularly at the longer wavelengths, comes from distributed emission.

Thus, we infer that the continuum against which we observe the interstellar dust extinction features is slightly concave upward, reflecting the increasing importance of IRS 1, which has a steeply rising spectrum, at the longer wavelengths (Rieke et al. 1978). Indeed, the increase in the curvature with aperture size, reflecting the increased importance of IRS 1, is quite apparent (compare the different panels in Fig. 1). Obviously, we cannot assume a simple (reddened) blackbody spectrum against which to measure the absorption features. Instead, we have adopted a "local" approach and assumed the linear continua across the absorption features indicated in Figure 1. Derived optical depth plots are shown in Figure 2. The error bars shown reflect only the statistical errors in the observations, and no

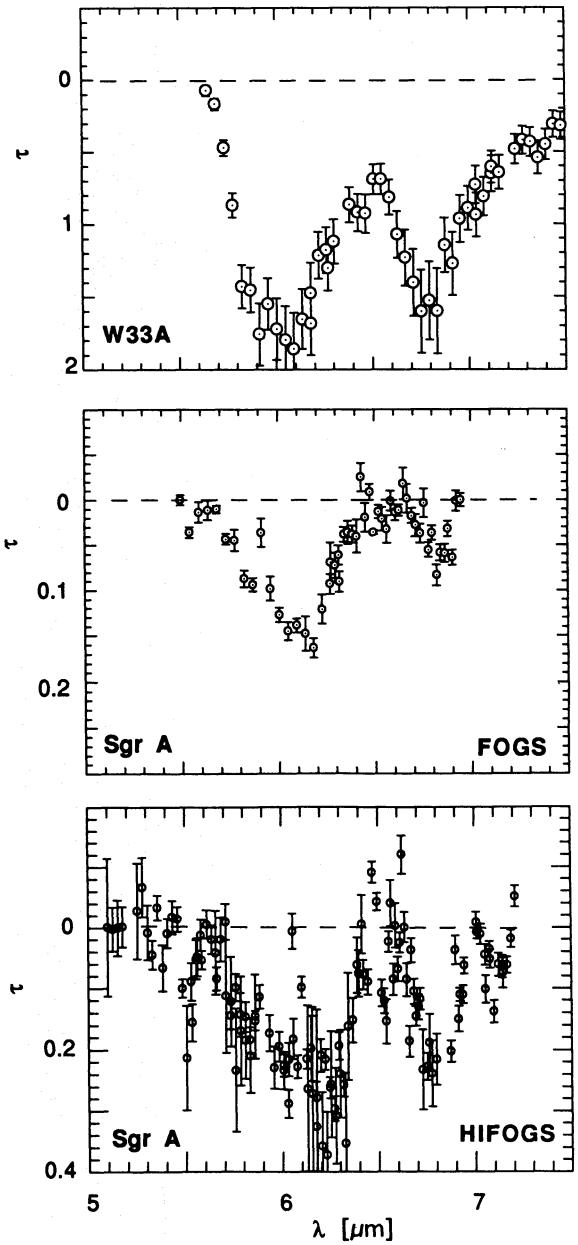

FIG. 2.—Absorption features in the 5–8 μm spectrum of the Galactic center derived from the medium-resolution FOGS (*middle*) and HIFOGS (*bottom*) data. For comparison the absorption spectrum measured toward the protostar W33A (Tielens 1989) is also shown (*top*).

allowance for the uncertainty in the adopted continua has been made. The derived optical depth in the HIFOGS data are about 0.05 larger than in the FOGS data due to differences in the adopted continua. However, the derived shapes of the absorption features are not much affected by this uncertainty.

3.2. *Dust Absorption Features*

The dust absorption features observed in the Galactic center spectrum are compared with those in the heavily obscured protostar W33A in Figure 2 (Tielens 1989). Clearly, while similar, the dust features do show differences in these two environments. In general, protostars show two broad ($\Delta\lambda \approx 0.5$ μm) features at 6.0 and 6.85 μm (Tielens & Allamandola 1987a). The Galactic center also shows quite broad ($\Delta\lambda \approx 0.5$ μm) absorption features around these wavelengths. However, the 6 μm feature is clearly centered at longer wavelengths, 6.1 rather than 6.0 μm. Moreover, the 6.1 μm feature in Sgr A is clearly asymmetric, with a wing to the short-wavelength side. The 6.1 μm features show very similar substructure in the FOGS and HIFOGS data. There is evidence for substructure at $\approx$5.8, 6.0, and 6.2 μm in both spectra that is not apparent in the spectrum of W33A. Even some of the narrow structure in the "continuum" between 6.4 and 6.7 μm repeats. The moderate-resolution FOGS spectrum of Sgr A shows some evidence for a weak and narrow absorption feature at about 7.6 μm, but this is not apparent in the HIFOGS data. This is a difficult part of the spectrum, even from airborne altitudes, due to telluric absorption. This feature may be due to interstellar solid CH_4 and will be discussed elsewhere (Boogert et al. 1995). The 5.5 μm band in the HIFOGS spectrum of Sgr A is not present in the spectrum of the protostar W33A.

4. IDENTIFICATION

IR spectra of sources in the Galactic center show a large number of absorption features (Butchart et al. 1986; Roche & Atiken 1985; Sandford et al. 1991; Pendleton et al. 1994; this paper). The characteristics of these features are summarized in Table 1. These features can be assigned to silicates, H_2O, CH_3, and CH_2 groups in saturated aliphatic hydrocarbons, and carbonyl (C=O) groups. Each of these carriers will be discussed in turn, and column densities will be derived.

4.1. H_2O

From its position and width, the 3.0 μm band can be attributed unambiguously to the OH stretching mode. Although the NH stretching mode also occurs in this spectral region ($\approx$2.96 μm), the NH stretching band is never as broad as the observed feature. Likewise, (much of) the 6.1 μm band can be assigned to the OH bending mode in H_2O. The peak position and shape of the 3.0 and 6.1 μm bands however, are inconsistent with the spectrum of pure amorphous or crystalline H_2O ice (Hagen, Tielens, & Greenberg 1981). Instead, the H_2O has to form part of an incompletely hydrogen-bonded network. Possible candidates are water of hydration in silicates (Tielens & Allamandola 1987b; Wada, Sakata, & Tokunaga 1991) and diluted mixtures of H_2O and other molecules with H_2O concentrations of $\approx$30% (Schutte & Greenberg 1988).

Minor amounts of water and OH ions are commonly found in minerals, even those normally considered to be anhydrous. Concentrating on water, H_2O can be present as isolated molecules, fluid inclusion (i.e., opal and feldspars), or in ordered crystalline structures (i.e., clays). Figure 3 shows a comparison between the 3.0 μm band in Sgr A IRS 7 (Sandford et al. 1991) and the OH stretching mode in water of hydration in talc (a hydrated magnesium silicate; Ferraro 1982) at room temperature. The comparison is quite reasonable. The discrepancy between the observed and experimental data shortward of 2.95 μm may indicate that the H_2O in the interstellar silicates forms part of a slightly larger hydrogen-bonded network than in the experiments. A similar good comparison between the interstellar 3.0 μm band and the spectrum of water of hydration in an SiO condensate has been presented by Wada et al. (1991). However, minerals such as serpentine or montmorillonite, dominated by "isolated" H_2O molecules or OH groups, do not provide good fits to the observed profile (Ferraro 1982).

The 3.0 μm band in the spectrum of Sgr A is equally well reproduced by a low-temperature grain mantle containing H_2O diluted by other molecules (Schutte & Greenberg 1988). In Figure 3, the observed spectrum is compared with the laboratory spectrum of a mixture of $H_2O/CO/NH_3/O_2$ (=0.32/0.23/0.13/0.32). A very good spectral match to the observations is evident. The main role of the CO and O_2 in this mixture is to break up the hydrogen-bonding network of the ice, while NH_3 produces a shoulder of absorption

TABLE 1

IDENTIFICATION OF ABSORPTION FEATURES IN THE SPECTRUM OF Sgr A

λ (μm)	ν (cm^{-1})	τ	$\Delta\nu$ (cm^{-1})	Identification	A[a] (cm molecule^{-1})	N (cm^{-2})	Reference
3.0	3300	0.63	450	H_2O	2 (−16)	1.4 (18)	1
3.38.....	2955	0.19	35	$-CH_3$	1 (−17)[b]	6.7 (17)	1
3.42.....	2925	0.19	30	$-CH_2-$	5 (−18)[b]	1.1 (18)	1
5.5	1820	0.12	30	$-CO-$[d]	2 (−17)	2 (17)	2
5.8[c]	1710	0.1	40	$-CO-$[d]	2 (−17)	2 (17)	2
6.1	1625	0.18	100	H_2O	8 (−18)	2.3 (18)	2
6.8	1460	0.16	20	$-CH_3$ and $-CH_2-$	1 (−18)[b]	3.2 (18)	2
(7.3)[e].....	(1380)	(0.02)	(10)	$-CH_3$	6 (−19)[b]	...	

[a] Intrinsic strength adopted from the compilation in Tielens et al. 1991.
[b] Strength for normal saturated aliphatic hydrocarbons adopted.
[c] This absorption refers to the short-wavelength wing present on the 6.1 μm feature.
[d] Carbonyl (C=O) stretching mode.
[e] Predicted to be present on the basis of the 3.38 μm feature.
REFERENCES.—(1) Sandford et al. 1991; (2) this paper.

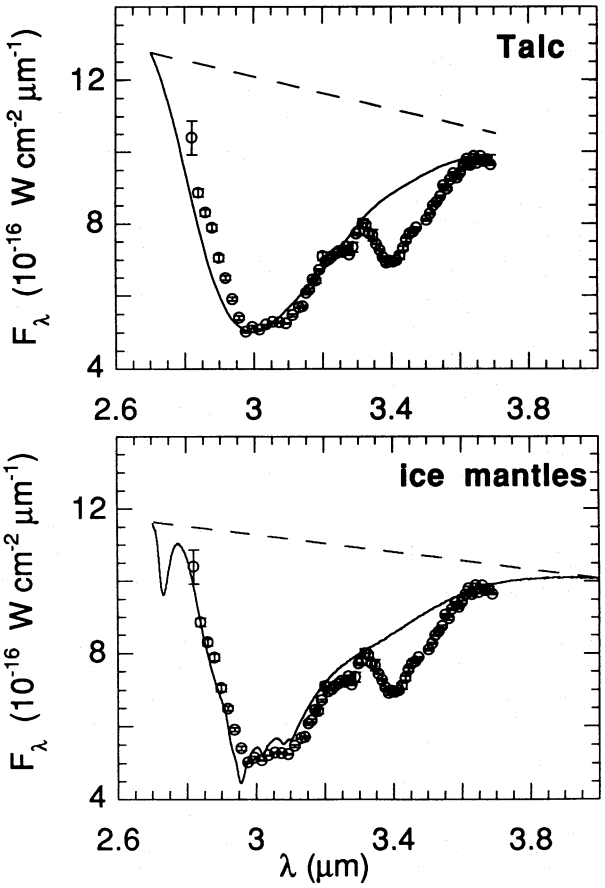

FIG. 3.—Absorption feature in the 3 μm spectrum of Sgr A IRS 7 (Sandford et al. 1991) is compared with the laboratory spectrum of talc, a hydrated silicate (*top*: Ferraro 1982), and with the spectrum of a mixture of H_2O:CO:NH_3:O_2 = 0.32:0.23:0.13:0.32 (*bottom*: Schutte & Greenberg 1988).

around 2.97 μm. Note also the weak band around 2.85 μm due to the OH stretching mode in H_2O molecules, in which one of the OH groups is not part of the H-bonding network. This is a very general characteristic of incompletely H-bonded H_2O ice mixtures.

The presence of the 6.1 μm OH bending mode confirms the identification of the 3.0 μm band with H_2O. Figure 4 compares the 6.1 μm band in Sgr A with the spectrum of talc and the H_2O mixture described above. These partially hydrogen-bonded networks have OH bending modes that peak slightly longward of the band in pure H_2O ice. The talc spectrum provides a reasonable fit to this feature. In contrast, the ice mixture does not provide a good fit at all. The good agreement in peak position of talc with the Sgr A spectrum provides further support for the identification of partially hydrogen-bonded H_2O networks. However, while the long-wavelength side of the 6.1 μm band is well reproduced, there is additional absorption shortward of 6 μm. This absorption is evident in all spectra (Figs. 1 and 2). This position is very characteristic for carbonyl stretches, and we propose this identification. This will be discussed further in § 4.3.

We have calculated the column density of H_2O in solid form along the line of sight toward Sgr A (Table 1). The intrinsic strength of the 3 μm OH stretching mode depends quite strongly on the degree of association (i.e., H-bonding) of the molecule. For H_2O the intensity of the OH stretch increases by a factor of about 500 in going from the isolated molecule to the fully hydrogen-bonded network of H_2O ice (van Thiel, Becker, & Pimentel 1957; Hagen et al. 1981 and references therein). The degree of association implied by the observations however, is high, and the strength of the 3.0 μm band is therefore not much less than for H_2O ice, and we have adopted that value (Hagen et al. 1981). The integrated strength of the 6.1 μm OH bending mode in H_2O is *not* sensitive to the degree of association, and we have used the value for pure H_2O ice (Hagen et al. 1981). The H_2O column densities calculated from the 3.0 and 6.1 μm bands agree reasonably well. Some discrepancy between the two values is expected, since the 3.0 μm band was measured with a much smaller beam than the 6.1 μm band, and the 3.0 μm band is known to vary on a 10″ size scale (McFadzean et al. 1989).

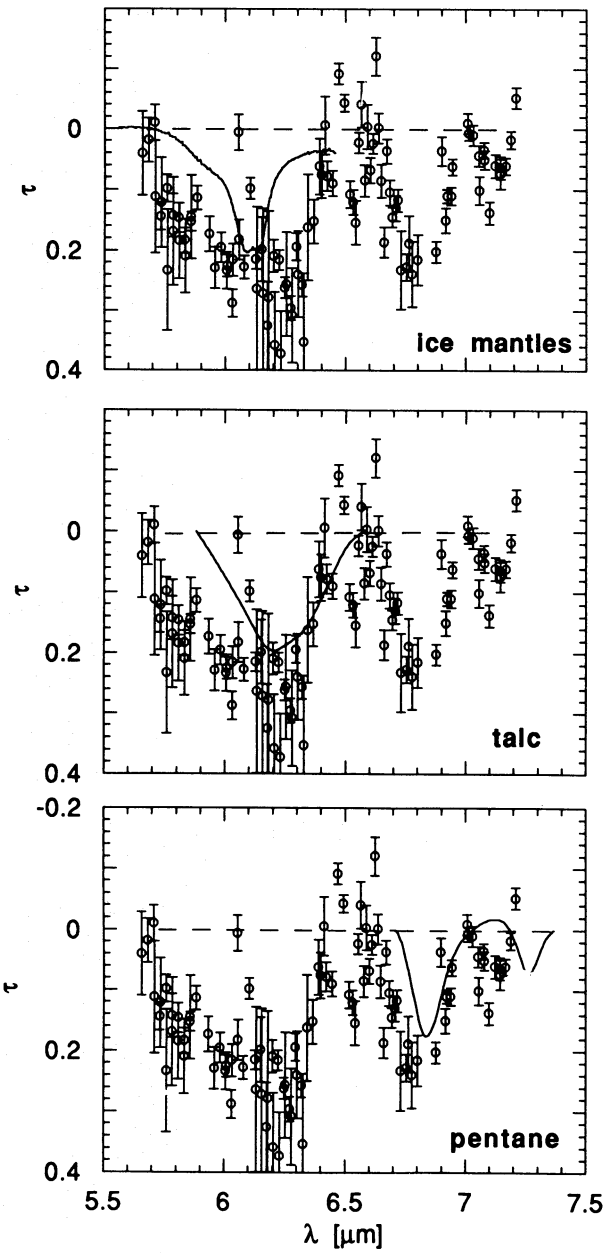

FIG. 4.—Absorption features in the spectrum of the Galactic center are compared with the laboratory spectrum of talc, a hydrated silicate (*top*; Ferraro 1982), with the spectrum of a mixture of H_2O:CO:NH_3:O_2 = 0.32:0.23:0.13:0.32 (*middle*), and with the laboratory spectrum of pentane (*bottom*).

While hydrated silicates provide a better fit to the 6.1 μm band of Sgr A, other arguments have been used in favor of the H_2O-rich ice identification. First, observations of several sources in the Galactic center region show that the depth of the 3.0 μm band varies considerably with position (McFadzean et al. 1989). For example, IRS 19, which is located about 20″ southeast of IRS 7, has an ice band optical depth of 3.6—about 5 times larger than IRS 7. In contrast, the near-IR and silicate extinction is fairly constant over the whole Galactic center region (Rieke, Rieke, & Paul 1989). Hence, the H_2O is localized to the Galactic center region. Second, Sgr A IRS 12 shows a weak 4.67 μm band due to solid CO (McFadzean et al. 1989). This unequivocally demonstrates that volatile ice grains exist along the line of sight toward the Galactic center region, likely existing in the molecular cloud associated with the Galactic center region (McFadzean et al. 1989). Third, in general, the 3 μm absorption feature has only been observed toward sources embedded in, or located behind, molecular clouds. Indeed, while Sgr A IRS 7 has $\tau(3\ \mu\text{m})/A_V = 0.027$, the upper limit for this ratio along the sight line to VI Cygni 12, which goes through the diffuse medium only, is 0.001. Fourth, the birth sites of interstellar silicates—oxygen-rich asymptotic giant branch (AGB) stars—do not as a rule show the 3 μm H_2O absorption feature.

While these arguments for ice are very compelling, they are not conclusive. In particular, examination of published 3 μm spectra of Galactic center sources (McFadzean et al. 1989) suggests that they consist of two independent components: (1) a broad component peaking at about 3 μm with a very pronounced long-wavelength wing, perhaps due to H_2O in silicates, and (2) a more "classical" ice band component that resembles the ice band observed in local protostellar spectra and is carried by H_2O ice. The 3 μm spectra of Sgr A IRS 3 and 19 are dominated by the former and latter component, respectively. In this view, the 6.1 μm band observed in our Galactic center spectrum of the IRS 3 region would be dominated by hydrated silicates, which provide a better fit to the observed feature. In any case, however, it should be borne in mind that this 3.0 μm band is only observed in Galactic center sources and is thus a characteristic of the inner galaxy. Sources such as VI Cygni 12 as well as the stellar birth sites of silicates do not show a 3.0 μm ice band. Hence, silicates in the local diffuse ISM are not hydrated.

One possible observational distinction between hydrated silicates and diluted ice mixtures is a band near 2.7 μm (3700 cm^{-1}). Diluted water ice mixtures show a weak band at this wavelength due to terminal OH, i.e., the OH stretch of "end" members of H-bonded structures that are not H-bonded to the rest of the ice structure (Hagen, Tielens, & Greenberg 1983). While hydrated silicates can show bands around this wavelength as well, not all hydrated silicates do (e.g., talc does not). If the 3 μm band in the Galactic center was the result of diluted H_2O ice, a band is expected around 2.7 μm with an optical depth of about 0.1 and a width of $\approx$0.04 μm. Present studies of this wavelength region are inhibited by strong telluric CO_2 absorption even from KAO altitudes. The *Infrared Space Observatory* (*ISO*) will, however, be able to test this assignment.

We recognize that the presence of multiple components may well be a more general property of 3 μm bands, even in local molecular clouds. Figure 5 shows a compilation of protostellar spectra (Smith, Sellgren, & Tokunaga 1989) selected to illustrate the presence of the classical 3 μm H_2O ice band component and the independent long-wavelength wing component.[3] Various carriers for the origin of this wing have been proposed, including scattering, overlapping hydrocarbon absorption features, and H_2O ice mixtures with a chemical base such as NH_3. All have some problems explaining the observations (cf. Tielens, Allamandola, & Sandford 1991). An origin of this wing in hydrated silicates is an interesting possibility, which is worth exploring further. If correct, the water of hydration must result from "wetting" in the ISM; a process which would be difficult to understand at the low temperatures prevalent.

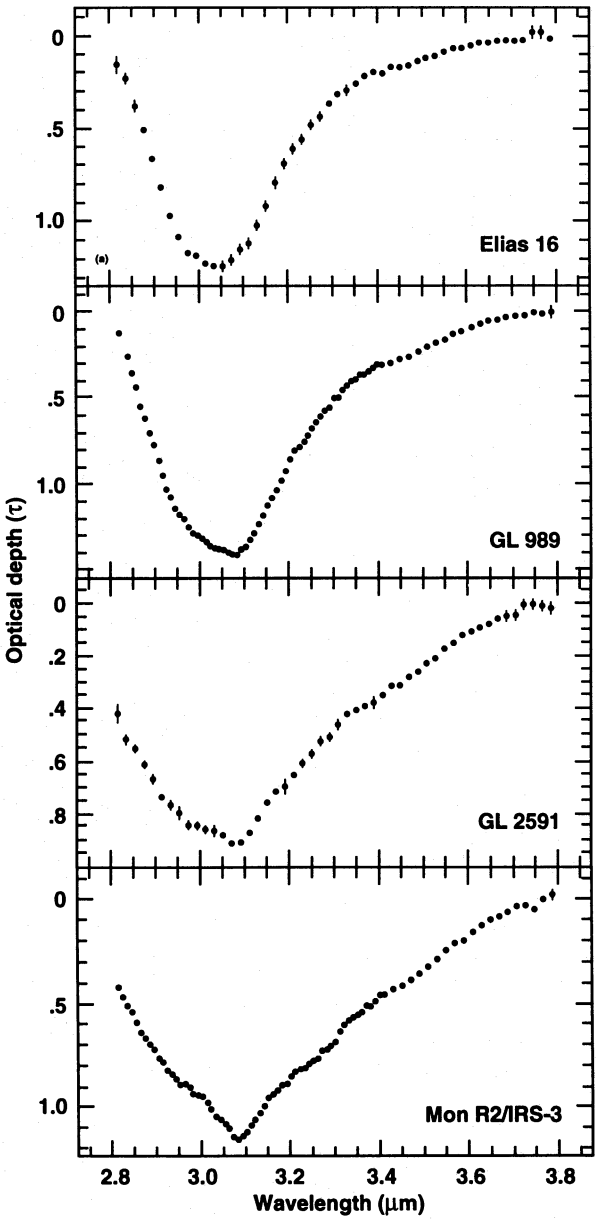

FIG. 5.—Variations in the shape of the 3 μm absorption feature in protostellar spectra may reveal the presence of an independent, long-wavelength wing component.

4.2. *Saturated Aliphatic Hydrocarbons*

The 3.4 μm region of the galactic center spectrum shows the unmistakable signature of solid aliphatic hydrocarbon

[3] The latter may also carry the spectral substructure around 2.95 μm.

molecules; the CH_2 and CH_3 symmetric and asymmetric stretching modes (Butchart et al. 1986; Sandford et al. 1991; Pendleton et al. 1994). However, while the peak positions of pure alkanes [$CH_3(CH_2)_nCH_3$] are close to the interstellar features, they do not fit in detail. An excellent fit to the interstellar spectrum is obtained for (some) aliphatic hydrocarbon molecules with slightly electronegative groups. Butanol [$CH_3(CH_2)_3OH$] is one example of such a molecule (Sandford et al. 1991). Kerogen, a complex mixture of organic molecules derived from organic remains, can also provide a good fit to the observed interstellar spectra (Ehrenfreund et al. 1991; Pendleton et al. 1994). Finally, from the substructure in the 3.4 μm band, the CH_2/CH_3 ratio in these organic molecules is 2.5 (Sandford et al. 1991; Pendleton et al. 1994).

The observed 5–8 μm spectrum of the Galactic center is consistent with this interpretation. Saturated aliphatic hydrocarbon molecules show CH_2 and CH_3 deformation modes at 6.8 and 7.3 μm (Bellamy 1960). The 6.8 μm band is clearly present in the observed spectrum (Fig. 2) and is well fitted by laboratory spectra of aliphatic hydrocarbon molecules (Fig. 4). The 7.3 μm band is intrinsically weaker than the 6.8 μm band by a factor of ≈ 2, and the observed spectra do not allow a meaningful comparison at that level.

The intrinsic strength of the CH stretching modes varies by more than a factor of 10 between different classes of aliphatic compounds, depending on the proximity of strongly electronegative substitutional groups within the molecule (Gribov & Smirnov 1962; Wexler 1967; d'Hendecourt & Allamandola 1986). However, the overall interstellar spectra reveal the presence of only weakly electronegative groups, and the strength of the CH_2 and CH_3 stretching modes in such molecules is very similar to those for pure aliphatic hydrocarbons. Hence, we have adopted the intrinsic strength of the latter (see Table 1). In our analysis, we have used the width of the observed features rather than the laboratory measured width for pure paraffins, and, as a result, our derived column densities are slightly larger than those derived before (Sandford et al. 1991; Pendleton et al. 1994). The integrated strength of the CH deformation modes is much less sensitive (by a factor of ≈ 2) to the molecular environment than the stretching modes. We have adopted the paraffin values, which are at the low range. The column density of CH_2 and CH_3 groups derived from the 6.8 μm region is somewhat larger than that derived from the 3.4 μm bands (3.2×10^{18} vs. 1.8×10^{18} cm^{-2}, respectively). This difference partly reflects the uncertainty in the placement of the continua and partly the uncertainty in the adopted intrinsic strength of these modes.

We note that the stretching and deformation modes of CH_2 and CH_3 groups close to strongly electronegative groups, such as ketones or esters, are comparable in intrinsic strength (Wexler 1967). In contrast, in pure aliphatics, the stretching modes are much stronger than the deformation modes. Since the 6.8 μm deformation band is observed to be much weaker than the 3.4 μm stretching bands in Sgr A, this, in addition to the difference in peak positions, rules out molecules such as esters and ketones as the carrier of the 3.4 and 6.8 μm bands.

Finally, unlike the OH stretching feature, which varies from source to source, the 3.4 μm absorption features are present in all Galactic center sources at the same strength (Pendleton et al. 1994). Also, the 3.4 μm feature has been seen in absorption along a variety of lines of sight in the Galaxy (Adamson et al. 1990; Sandford et al. 1991; Pendleton et al. 1994). Hence, aliphatic hydrocarbons are a component of the dust in the diffuse interstellar medium and not just local to the Galactic center.

4.3. *Carbonyl Groups*

4.3.1. *The 5.8 μm Wing*

As discussed in § 4.1, the short-wavelength side of the 6 μm feature is not well fitted by the OH deformation mode of H_2O. We attribute the additional absorption centered at 5.8 μm to carbonyl (C=O) groups in organic molecules. This position is very characteristic for such groups (cf. Table 2). The peak position is somewhat dependent on substitution, varying from ≈ 5.5 to 5.9 μm (Table 2). It is tempting to identify the observed substructure in this wing to the presence of a variety of carbonyl-bearing molecules, including saturated ($\lambda_{peak} \approx 5.85$ μm) and unsaturated ($\lambda_{peak} \approx 5.6$ μm) ketones and aldehydes. However, the presence of the strong H_2O bending mode at 6.1 μm severely hinders this interpretation, and a detailed identification has to await further higher resolution observations. The intrinsic strength of the carbonyl band varies by a factor of 3 (Wexler 1967). We have adopted a value in the midrange (see Table 1). The peak strength of the CH stretching and bending modes of CH_2 and CH_3 groups close to the strongly electronegative C=O group are very weak, and, based upon the observed C=O column density, predicted peak optical depths for these bands are ≈ 0.02 and presently unobservable.

4.3.2. *The 5.5 μm Band*

The 5.5 μm (1820 cm^{-1}) feature occurs in the region of the strong carbonyl (C=O) stretching vibration, which is otherwise devoid of strong absorption bands (Bellamy 1960). However, this wavelength is rather unique, and simple ketones, carboxylic acids, or aldehydes are excluded (cf. Table 2). Instead, this wavelength may indicate a carbonyl group either close to a halocarbon group (e.g., Cl) or in a metal carbonyl [e.g., $Fe(CO)_4$] (cf. Table 2). Halocarbon groups seem excluded because of abundance considerations.[4] If carried by dust in the diffuse medium, about 1% of the elemental Fe would have to be locked up in iron

[4] For a column of $N_H \approx 10^{23}$ cm^{-2} a halogen abundance greater than 2×10^{-6} is required (cf. § 5 and Table 1).

TABLE 2

CARBONYL STRETCHING FREQUENCIES IN THE 5–8 μm REGION

Compound	Structure[a]	ν (cm^{-1})	λ (μm)
Ketones	R—CO—R	1706	5.86
Aldehydes	R—CO—H	1719	5.82
Carboxylic acid	R—CO—OH	1778[b]	5.62[b]
Esters	R—CO—O—R	1738	5.75
Metal carbonyl	Fe $(CO)_4$	1833	5.46
Organic peroxide	R—CO—O—O—CO—R	1813	5.52
		1786	5.60
Acid halide	R—CO—X	1810	5.52
Radical	HOCO	1832	5.46
Radical	HCO	1860	5.38

[a] Structure of the compound in terms of molecular groups: CO = carbonyl group (C=O), R = aliphatic group (combinations of CH_2 and CH_3 groups), X = halogen group.

[b] Monomer frequency measured in a N_2 matrix.

carbonyl groups to explain the observed 5.5 μm band. If this species were part of the ice mantles localized in the Galactic center region itself, this value would be much higher. Absorptions in the 5–6 μm region are also characteristic for carbonyl groups in acid anhydrides (—CO—O—CO—) and organic peroxides (—CO—O—O—CO—). However, these species show a pair of bands separated by 0.08–0.15 μm in this spectral range and can therefore be excluded.

The carbonyl stretch in radicals is also shifted to higher frequencies. HOCO, for example, absorbs at 5.46 μm (1832 cm^{-1}), close to the interstellar peak position. Laboratory experiments on UV photolysis of H_2O/CO mixtures at low temperatures produce this radical through the reaction of CO and OH. Other unidentified absorption bands also appear upon photolysis in this wavelength region (Milligan & Jacox 1971; Hagen 1982). However, these photolysis experiments produce much more HCO through the reaction of H with CO. HCO absorbs at 1860 cm^{-1} (5.38 μm), and there is no sign of that band in the Galactic center spectrum. Hence, the identification of the 5.5 μm band with HOCO and similar radicals is less likely than the identification with metal carbonyls.

5. THE COMPOSITION OF INTERSTELLAR DUST

The column densities derived in the previous section (Table 1) can be compared with those of other interstellar dust components. Also, once we have estimated the total H-column density along the line of sight, we can derive the fraction of an element locked up in a dust component and the total volume of that dust component per H atom using (Tielens & Allamandola 1987b)

$$V_j = \frac{1}{\rho_s} \sum_i f_{ij} A_i m_i ,$$

where ρ_s is the specific density of dust component j, f_{ij} is the fraction of element i locked up in dust component j, and A_i and m_i are the cosmic abundance and mass of element i, respectively. The results for various dust components identified in the ISM are compared in Table 3.

5.1. *Silicates*

The 9.7 and 18 μm Si—O stretching and bending modes of interstellar silicates have been observed toward the Galactic center (Roche & Aitken 1985). Using $N_H/\tau(9.7\ \mu m)$ determined for the local solar neighborhood (3.5×10^{22} H atoms cm^{-2}; Roche & Aitken 1984), these silicate observations translate into a column density of H atoms of $\approx 10^{23}$ cm^{-2}. If we had started with the visual extinction ($A_V = 30$ mag), estimated from the near-IR extinction, then the total H-column density would be somewhat less, $\approx 6 \times 10^{22}$ cm^{-2}. This difference merely reflects the enhanced $\tau(9.7\ \mu m)/A_V$ ratio toward the Galactic center as compared with the solar neighborhood (Roche & Aitken 1985). A similar enhancement has been observed for the $\tau(3.4\ \mu m)/A_V$ ratio toward the Galactic center (Pendleton et al. 1994). Likely, therefore, these variations result from a decrease in the near-IR (and visual) extinction per unit dust (or gas) mass in the Galactic center region. Such a decrease in the near-IR extinction may result, for example, from an increase in grain size. This would imply that grains in the direction of the Galactic center have sizes ≥ 0.3 μm ($a \geq \lambda/2\pi$). In the subsequent discussion, we will convert all observed dust column densities to abundances using the former value for the H-column density. The 9.7 μm SiO stretching band is a good measure of the column density of Si atoms locked up in silicates along the line of sight toward the Galactic center (Table 3; Tielens & Allamandola 1987b). This column density has been translated into a silicate dust volume per H atom using a specific grain density of 2.5 g cm^{-3}, typical for amorphous silicates, and assuming a stoichiometric composition of (Mg, Fe)SiO_4.

5.2. *The Hydrocarbon Component*

Assuming solar abundances (Anders & Grevesse 1989), we estimate that ~0.08 of the elemental C and a negligible fraction (0.005) of the elemental O are depleted in hydrocarbon grains (Table 3). This is less than originally estimated by Tielens & Allamandola (1987b; 0.24 of the C and 0.06 of the O). Part of this difference results from the difference in the assumed H-column density; the earlier study normalized to the H-column density derived from the near-IR colors. Furthermore, the earlier work adopted the smaller intrinsic strength for the CH stretching mode appropriate for small alcohols (e.g., methanol). Given that the peak positions of the interstellar 3.4 μm bands are hardly disturbed from those for pure alkanes, the presently adopted value is

TABLE 3

COMPOSITION OF INTERSTELLAR DUST

Component (1)	Element (2)	N^a (10^{18} cm^{-2}) (3)	Abundance[b] (4)	Volume (10^{-27} cm^3) (H atom)$^{-1}$ (5)
Hydrocarbons.....	C	3.2	0.08	0.7
Silicates	Si	3.8	1.0	4.3
graphite[c]	C	...	0.16	0.5
PAHs[d]	C	...	0.01	0.03
HAC[e]	C	...	0.08	0.3
SiC	C	<0.2	<0.006	<0.04
Al_2O_3	Al	<0.2	<0.8	<0.04
Total	...	...	...	7.0

[a] Column density toward Sgr A of element identified in column (2).
[b] Fraction of the elemental cosmic abundance locked up in this dust component.
[c] Values are based upon the 2200 Å extinction bump in the local ISM.
[d] Values determined from the IR emission spectra of the local ISM.
[e] Values estimated from the ERE. This component may actually be the same as the hydrocarbon component.

the best choice. Indeed, we note that larger alcohols, which have CH stretching modes close to those of pure alkanes, also have the same intrinsic strengths as alkanes. Finally, it is now known that the OH stretching mode at 3 μm is not associated with the hydrocarbon component (McFadzean et al. 1989; Sandford et al. 1991; Pendleton et al. 1994). The derived elemental fractions locked up in hydrocarbon grains are converted into grain volumes using a specific grain density of 1 g cm^{-3}, typical for organic solids.

Strictly speaking, the 3.4 and 6.8 μm bands probe only the C—H bonds in saturated aliphatic hydrocarbon materials. The C—H stretching vibrations of CH_2 and CH_3 groups close to highly electronegative groups, such as C=O and CN, are intrinsically much weaker and difficult to detect. We have estimated the column density of C=O groups from the observed structure near the C=O stretch at 5.8 μm (§ 4.3 and Table 1). Twice that column density could be in the form of CH_2 and CH_3 groups close to these C=O groups and hence "hidden" from our view. That would add another 0.01 to the fraction of the elemental C locked up in hydrocarbon grains. The abundance of nitrile groups, which absorb in the middle of the telluric CO_2 band, will have to await the launch of *ISO*.

5.3. *Graphitic Dust*

Aromatic hydrocarbons have intrinsically very weak CH stretching vibrations, $\approx$0.1 of the aliphatic CH stretch on a per C-atom basis. The observed upper limit on the aromatic C—H stretching mode in absorption toward Sgr A corresponds to a fraction of about 0.01 of the elemental C (Pendleton et al. 1994). The 3 μm spectrum of the protostar Mon R2 IRS 3 reveals a weak absorption feature at 3.25 μm that also corresponds to $\approx$0.01 of the elemental C locked up in aromatic hydrocarbons (Sellgren et al. 1995). The IR *emission* spectrum of the ISM reveals that the fraction of elemental C locked up in molecular (20–100 C atoms) aromatic structures [i.e., polycyclic aromatic hydrocarbons (PAH) molecules] is about 0.01 with a typical C/H ratio greater than 2 (Allamandola, Tielens, & Barker 1989). The fraction of C locked up in larger PAHs, PAH clusters, and small aromatic grains is $\approx$0.1 (Tielens 1990), but their C/H ratio is much larger and they will not contribute much to the CH stretching vibration. Hence, the absorption upper limit is reasonably consistent with the estimate from IR emission observations. We have estimated the fraction of the C in the form of PAHs from the IR emission spectrum of the ISM. The value reported in Table 3 corresponds only to the IR emission features at 3.3, 6.2, 7.7, and 11.3 μm themselves and not to the underlying plateaus or the 12 and 25 μm *IRAS* observations. These other components are carried by much larger units (100–1000's of C atoms rather than $\approx$50 C atoms; Tielens 1990). This abundance has been translated into a molecular PAH volume using the graphite-specific density of 2.2 g cm^{-3} (Table 3), corresponding to an assumed thickness of these planar molecules of 3.5 Å, the interlayer spacing of graphitic sheets.

A large fraction of the elemental carbon may be contained in graphite or amorphous carbon grains. Attributing the 2200 Å feature to small (<200 Å) graphite grains, 0.16 of the elemental carbon is locked up in such grains (Draine 1989). Larger graphite grains do not show pronounced UV features (Draine & Lee 1984). The 11.52 μm graphite feature is too weak and narrow to provide a meaningful estimate of the interstellar graphite abundance (Draine 1984). Hence, at present, we can only speculate about the fraction of the elemental C locked up in large graphite grains. Estimates range from none (Greenberg & Chlewicki 1984) to about 0.60 (Mathis et al. 1977; Draine & Lee 1984). Table 3 summarizes only the directly observed graphite dust volume derived from the 2200 Å bump, assuming a specific density of 2.2 g cm^{-3}.

5.4. *Hydrogenated Amorphous Carbon*

Hydrogenated amorphous carbon (HAC) grains (H/C > 0.5) will show IR absorption features due to aliphatic CH_2 and CH_3 modes at 3.4 and 6.8 μm. Under some conditions, HAC can provide a good fit to the observed 3.4 μm band as well. The interstellar HAC abundance corresponds then to 0.05 of the elemental C, derived above for the carrier of the 3.4 μm feature (with an H/C of 2.3 corresponding to $CH_2/CH_3 = 2.5$). Adopting an H/C ratio as low as 0.5 would increase that estimate by a factor of $\approx$5 for the "unseen" C (i.e., not bonded to H). However, most of the H in HAC with such low H/C values is aromatically bonded rather than aliphatically bonded (Angus, Koidl, & Domitz 1986; Robertson 1986), and spectra of such HAC materials do not provide a good fit to the observed interstellar spectra.

Independent constraints on the interstellar HAC abundance result from observations of the extended red emission (ERE). The ERE is a broad luminescence band observed in reflection nebulae, H II regions, and planetary nebulae (Schmidt, Cohen, & Margon 1980; Witt & Schild 1986; Furton & Witt 1992). HAC luminesces when exposed to FUV photons, and the laboratory measured HAC feature fits the observed ERE band well (Duley & Williams 1988; Furton & Witt 1993). ERE-to-scattered light intensity ratios measured in reflection nebulae are typically 0.1 (Witt & Boroson 1990). We will derive the fraction of elemental C locked up in HAC from this intensity ratio observed in the well-known reflection nebula, NGC 2023, assuming that the ERE is pumped by FUV photons. With a stellar red-to-FUV photon flux ratio of 0.11, and standard dust extinction and scattering properties, the fraction of the FUV extinction due to HAC is given by $f_{HAC} = 0.002/Y$, where Y is the yield per FUV photon. With an average FUV absorption cross section of 10^{-17} cm^2/C-atom and $\tau(\mathrm{FUV})/N_H = 1.6 \times 10^{-21}$ cm^2, the fraction of the elemental C locked up in HAC is $0.4 f_{HAC} \approx 0.0008/Y$. Measured HAC luminescence yields excited by 4600 Å photons are 0.002 at room temperature (Furton & Witt 1993). This yield is likely to increase with decreasing temperature but decrease with increasing FUV photon excitation energy. Here, we adopt a yield of 0.01, corresponding to 8% of the elemental C in the form of HAC. This abundance is chosen to be the same as for the carrier of the 3.4 μm feature since we surmise that they are one and the same material. We note that the luminescence yield of the ERE carrier cannot be less than 0.002, corresponding to all of the elemental C and essentially all of the FUV extinction.

5.5. *Other Refractories*

Silicon carbide, diamond, graphite, and aluminium oxide grains with isotopic compositions revealing an origin in stellar outflows have been isolated from meteorites supporting the presence of these types of grains in the ISM (Huss et al. 1994; Hutcheon et al. 1994; Zinner et al. 1995; Lewis et al. 1987). SiC dust grains have been observed in emission in

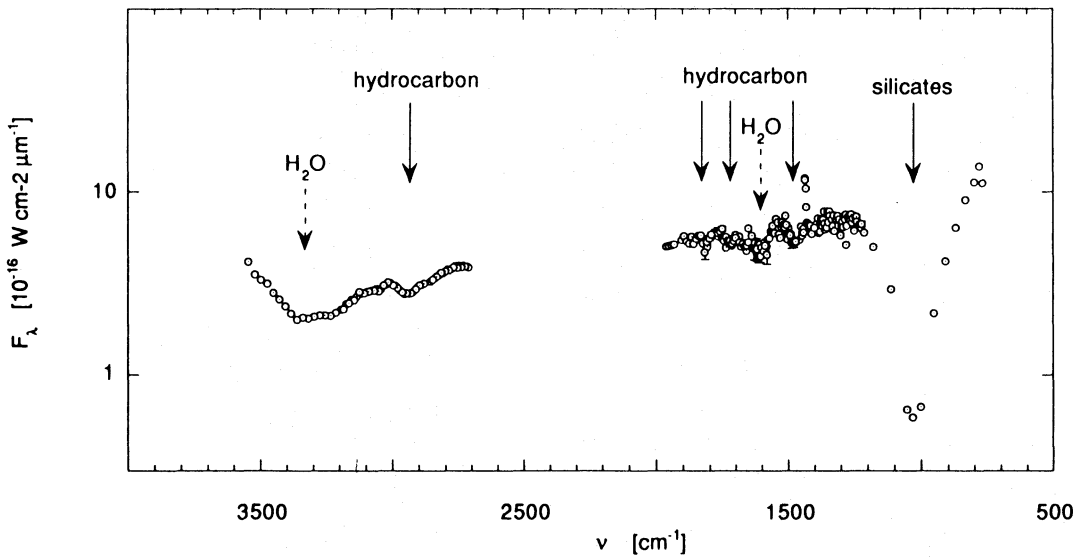

FIG. 6.—IR spectrum of interstellar dust. Absorption features in the spectrum of the Galactic center. Arrows identify absorption bands due to the various dust components. Except for the 3 μm H_2O band, the integrated strength per unit dust volume of the various bands are quite comparable. Hence, on this τ-scale, equal areas of absorption features indicate equal volumes of the interstellar dust components responsible.

circumstellar dust shells around C-rich giants but never in absorption in the ISM. Whittet, Duley, & Martin (1990) have estimated an upper limit of less than 2×10^{17} C atoms cm^{-2} in SiC grains toward the Galactic center from the absence of the 11.2 μm SiC stretch. This corresponds to less than 0.006 of the elemental C (and, similarly, less than 0.06 of the elemental Si) in the form of SiC grains. A specific density of 3 g cm^{-3} has been assumed for SiC in Table 3.

Al_2O_3 grains have been identified in the IR emission spectrum of certain types of O-rich giants (Vardya, de Jong, & Willems 1986; Onaka, de Jong, & Willems 1989). The 13 μm band due to such grains has never been observed in absorption in the ISM. The upper limit to the column density of Al involved in interstellar grains is similar to that for C in SiC derived above. However, because of the low cosmic abundance of Al, the upper limit on the fraction of the Al in such grains is not very restrictive (0.8). A specific density of 4 g cm^{-3} has been assumed.

Various protostellar spectra show an absorption feature at 3.47 μm that has been attributed to the CH stretching vibration in tertiary H (i.e., aliphatic C with only one H attached; Allamandola et al. 1992). This could be H peripheral groups on the surfaces of interstellar diamond grains. However, recent studies suggest that this absorption feature is limited to molecular cloud material and hence is not a component of the dust in the diffuse medium (Brooke, Sellgren, & Smith 1995). Present observational limits on the abundance of diamond grains in the diffuse medium are not very restrictive (Lewis, Anders, & Draine 1989).

5.6. *Discussion*

The total dust volume can be estimated from a Kramers-Kronig analysis of the interstellar extinction curve (Purcell 1969). This yields $\approx 7 \times 10^{-27}$ cm^3 (H-atom)$^{-1}$ (Spitzer 1978).

Comparing the observed dust volumes, we conclude that the organic component of the interstellar dust accounts for only a small fraction (0.1) of the total dust volume. In contrast, silicate grains are known to contribute 60% of the interstellar dust volume. This disparity is directly obvious from the observed IR absorption spectrum of interstellar dust (Fig. 6), which is dominated by the 10 μm silicate band despite the fact that the integrated intrinsic strength per unit dust volume of the hydrocarbon band is very similar to that of the silicate band. The interstellar dust volume due to small graphite grains is somewhat smaller than that of hydrocarbon dust grains. All other identified dust components contribute negligibly to the interstellar dust.

The total volume in identified dust components is only 0.75 of the total dust volume required to explain the visible and UV extinction. From cosmic abundances and elementary chemistry, it is clear that the missing dust mass is largely carbonaceous in nature. Indeed, models with less than 65% of the carbon in solid form cannot reproduce the observed interstellar extinction curve (Mathis 1995).[5] From our observations it follows that the dust component does not have strong IR absorption bands. Large graphite, diamond, or amorphous carbon grains are obvious candidates. Graphite is a semimetal, and its IR spectrum is dominated by electronic interband transitions. Large graphite grains also show no discernible UV feature (Draine & Lee 1984). Diamond is a perfect monovalent crystal and consequently has no active IR modes. Disorder will introduce some IR activity, and amorphous diamond grains will show weak and broad absorption near the peak in the phonon density of states (≈ 5 μm), which will be difficult to detect. Surface functional groups will show IR activity, but for large grains their number will be small. The onset of the UV band edge near 1800 Å is also difficult to detect, even if all of

[5] Recent measurements suggest that B stars, and by inference the interstellar gas from which they were recently formed, have a C-elemental abundance much less than solar, completely insufficient to explain the observed interstellar extinction curve (cf. Mathis 1995). We would hold that either these abundance studies contain large systematic errors, e.g., due to non-LTE effects, or the premise that they represent interstellar abundances is incorrect, e.g., due to incomplete incorporation of dust in massive protostars (cf. Yorke 1996).

the elemental C is locked up in such grains (Lewis et al. 1989). If all of the elemental C were locked up in diamonds, such grains would only dominate the interstellar extinction below 1000 Å, where the extinction curve is poorly constrained observationally. The IR spectrum of amorphous carbon (or highly dehydrogenated HAC) will also show C—C stretching vibrations in the range 7.5–8 μm. With an estimated integrated intrinsic strength of 3×10^{-19} cm (C atom)$^{-1}$ and a width of 100 cm^{-1}, 0.2 of the C in such grains corresponds to an optical depth toward the Galactic center of 0.02. At present this cannot be excluded from the observations.

6. ORIGIN OF THE INTERSTELLAR HYDROCARBON DUST COMPONENT

The 3.4 μm absorption feature is generally not observed in the spectra of stardust birth sites such as carbon giants. As a result, models for this dust component concentrate on a truly interstellar origin (i.e., formed in the ISM). Perhaps the most striking aspect of the composition of the hydrocarbon component of the interstellar dust derived here is its apparent simplicity. Interstellar hydrocarbon dust is dominated by CH_2 and CH_3 groups in saturated aliphatic hydrocarbons with small amounts of carbonyl (C=O) groups. Some OH groups may also be part of this component, their bands hidden underneath the 3.0 μm H_2O band. This apparent simplicity poses some strict limits on the chemistry involved in their production.

It has been suggested that the hydrocarbon component of the interstellar dust results from UV photolysis and warm-up of icy grain mantles accreted in dense clouds (Greenberg 1979). Extensive laboratory studies show that these processes transform a small fraction ($\approx$1%) of the initial mixture into a refractory organic residue (Hagen, Allamandola, & Greenberg 1979; d'Hendecourt et al. 1986; Schutte 1988; Allamandola, Sandford, & Valero 1988; Jenniskens et al. 1993). Most studies have been performed on initial mixtures rich in H_2O, and, generally, their IR spectra show only a weak 3.4 μm band. Accordingly, the measured IR spectrum of organic residues produced by FUV photolysis does not provide a good fit to the observed spectrum of the Galactic center. In particular, these photolysis residues show C=O stretching modes around 5.8 μm that are much stronger (relative to the CH stretching modes) than observed. The same holds for the IR spectra of kerogens (Ehrenfreund et al. 1991). Hence, in contrast to the materials studied in the laboratory, interstellar hydrocarbon grains consist just of hydrogen and carbon with very little oxygen (cf. Table 1). Perhaps prolonged exposure to the interstellar FUV radiation field will lead to an almost complete carbonization of the interstellar residue and a consequent loss of all chemical memory (Tielens 1989). There is some laboratory support for such a view (Jenniskens et al. 1993). In that case, the chemical structure of these organic residue mantles would resemble that of HAC.

Alternatively, it has been speculated that HAC grain mantles might condense directly on preexisting grain cores in the diffuse ISM (rather than in molecular clouds; Jones, Duley, & Williams 1990; Duley 1993). Laboratory studies show that HAC will indeed condense from a warm plasma that is rich in H and C (Angus et al. 1986). However, the detailed astrochemical route that forms HAC at 10 K, rather than H_2O-rich ices in a gas that is rich in H and O, is difficult to imagine. It is likely that this growth process, if at all possible, is very inefficient, particularly since both the dust grains and the gaseous carbon will be positively charged in the diffuse ISM. Perhaps the hydrocarbon interstellar dust component may not reflect mantle growth in the ISM at all but rather the modification of an existing dust component. Furton & Witt (1993) have shown experimentally that amorphous carbon will transform to HAC under exposure to (thermal) atomic H, particularly in the presence of strong UV fields. In this case, accreting thermal atomic H reacts with radical sites created by the UV irradiation process. Since atomic H is so overabundant in the diffuse ISM, little carbon grain growth is expected this way. Likewise, proton bombardment of graphitic, amorphous carbon, or diamond surfaces in interstellar shocks will lead to the formation of a 10–20 Å surface layer of HAC through ion implantation (Tielens et al. 1994). Such shocks occur frequently enough (a 100 km s^{-1} shock every $\approx 10^8$ yr; Jones et al. 1994) to rapidly convert essentially all carbonaceous grain surfaces to HAC. In the latter two models, the OH and C=O groups present in the interstellar hydrocarbon dust component would reflect traces of oxygen incorporated into the structure during the modification process.

The difference between these models is largely driven by a different view on the global evolution of interstellar dust. Models in which interstellar dust is dominated by stardust injection from AGB stars and supernovae might look toward surface modifications as the origin for hydrocarbon compounds. Models in which most of the dust is formed in the ISM attribute the hydrocarbon features to accreted grain mantles. In evaluating these competing models, two additional points have to be considered. First, theoretical studies show that interstellar dust is rapidly destroyed by strong shocks. This is supported by observational studies of elemental depletions as a function of cloud velocity, which show almost solar abundances at high velocities. The calculated dust lifetime, 0.5 Gyr, is much less than the injection timescale for stardust (Jones et al. 1994). Hence, dust has to be (re-)formed rapidly in the ISM.

Second, the 3.4 μm absorption feature is absent in sight lines through molecular clouds (Allamandola et al. 1993). All of the models discussed above face some problems explaining this property. Typically, the lifetime of molecular clouds against complete disruption by newly formed massive stars is $\approx 3 \times 10^7$ yr. Hence, over the Galactic lifetime of a dust grain, 3×10^8 yr (Jones et al. 1994), a dust grain will cycle back and forth several times between the molecular cloud phase and the diffuse medium phase. The absence of the 3.4 μm absorption features in the spectra of protostars suggests, then, that the hydrocarbon component of interstellar dust is rapidly destroyed or converted back to amorphous carbon inside dense clouds. Annealing of HAC at temperatures in excess of $\approx$800 K leads to H loss and amorphous carbon formation (de Vries 1987; Angus et al. 1986). Likewise, UV photons in the absence of H can drive off aliphatic H and convert HAC into amorphous carbon (Duley 1993; Furton & Witt 1993). However, neither of these processes is expected to be important in molecular clouds. Dust temperatures are generally very low in the ISM unless the grains are very small ($\approx$50 C atoms). Also, if anything, the ratio of the UV flux to atomic H flux is less by many orders of magnitude inside dense clouds than in the diffuse medium. Likewise, dust destruction by shocks is expected to be more important in the diffuse medium than in molecular clouds (Seab 1987; McKee 1989). Hence, the

absence of hydrocarbon dust inside dense molecular clouds remains enigmatic to all models.

Obviously, a variety of processes can be envisioned that lead to the formation of a hydrocarbon material in the diffuse ISM. Which of these dominates, if any, is presently not known. All of them face some problems. Nevertheless, the consensus developing in the literature, partly driven by observations, that a material like (slightly oxidized) HAC is present in the interstellar dust is perhaps not surprising given the highly reducing conditions of interstellar space and the inherent stability of aromatic carbon structures.

7. SUMMARY

The IR spectrum of the Galactic center shows absorption features at 3.0, 3.4, 5.5, 5.8, 6.1, 6.8, 9.7, and 18.2 μm. The 3.0 and 6.1 μm features are due to the OH stretching and bending modes in H_2O. Equally good fits to the observed 3 μm spectra can be obtained with diluted ice mixtures containing approximately 30% H_2O and with hydrated silicates (e.g., talc). The observed 6.1 μm band however, is, better fitted by hydrated silicates. We suggest that the 3.0 μm band observed toward Galactic center sources consists of two components: (1) a broad feature with a prominent long-wavelength wing carried by hydrated silicates, and (2) a narrower 3 μm band resembling that observed in "local" protostars due to H_2O ice. The latter component is local to the molecular cloud in the Galactic center region. The presence of more than one component may be a more general property of interstellar 3 μm features. The features near 3.4 and 6.8 μm are due to the stretching and deformation vibrations of CH_2 and CH_3 groups in saturated aliphatic hydrocarbons close to weakly electronegative groups. The 5.5 and 5.8 μm bands are attributed to the carbonyl (C=O) stretching vibration. Likely, the 5.5 μm band is due to metal carbonyls [i.e., $Fe(CO)_4$]. Finally, the 9.7 and 18.2 μm bands are due to silicates.

The 3.4 μm band is well fitted by a variety of hydrocarbon materials, including organic residues produced by FUV photolysis and kerogen. The 5–8 μm spectra of laboratory-produced organic residues (and of kerogen) are dominated by the strong C=O stretching mode around 5.8 μm. In contrast, the IR spectrum of the Galactic center reveals that interstellar solid hydrocarbon grains contain very little oxygen. In that respect, they resemble HAC-like materials.

Abundances have been derived for various proposed interstellar dust components. Comparing these, we conclude that hydrocarbon grains are only a minor component of the interstellar dust, contributing ≈ 0.1 to the total dust volume. About 0.6 of the interstellar dust volume is in silicate grains. Small graphite grains, responsible for the 2200 Å bump, contribute 0.07 of the dust volume. Other identified dust components are negligible. Hence, about 0.25 of the interstellar dust volume is presently unaccounted for in the IR. Likely, this dust consists of large graphite, diamond, or amorphous carbon grains that have weak or no IR active vibrational modes.

Various models have been proposed for the origin of the hydrocarbon dust component in the ISM. These include grain-growth schemes either by accretion of an ice mantle inside dense clouds followed by UV photolysis and warm-up, or by direct accretion of a hydrogenated amorphous carbon mantle in the diffuse medium. Alternatively, the hydrocarbon dust component may signal the modification of a preexisting dust component, probably amorphous carbon, rather than a grain-growth process, through thermal reactions with atomic hydrogen or through ion implantation in fast shocks. All of these processes face some problems in explaining all of the observations, particularly the absence of the hydrocarbon dust component in the shielded environments of molcular clouds.

This study would not have been possible without the dedication and effort of the entire KAO crew. We thank John Mathis for an ongoing dialog on the mysteries of interstellar dust. Studies of interstellar dust at NASA Ames Research Center are supported under NASA's Airborne Astronomy Program, RTOP 352-02-03-06, and through the NASA Astrophysics Theory Program, RTOP 399-20-10-27.

REFERENCES

Adamson, A. J., Whittet, D. C. B., & Duley, W. W. 1990, MNRAS, 243, 400
Allamandola, L. J., Sandford, S. A., Tielens, A. G. G. M., & Herbst, T. M. 1992, ApJ, 399, 134
———. 1993, Science, 260, 64
Allamandola, L. J., Sandford, S. A., & Valero, G. J. 1988, Icarus, 76, 225
Allamandola, L. J., Tielens, A. G. G. M., & Barker, J. R. 1989, ApJS, 71, 733
Allen, D. A., & Wickramasinghe, D. T. 1981, Nature, 294, 239
Anders, E., & Grevesse, N. 1989, Geochim. Cosmochim. Acta, 53, 197
Angus, J. C., Koidl, P., & Domitz, S. 1986, in Plasma Deposited Thin Films, ed. J. Mort & F. Jansen (Boca Raton: CRC Press), 89
Becklin, E. E., Mathews, K., Neugebauer, G., & Willner, S. P. 1978a, ApJ, 219, 121
———. 1978b, ApJ, 220, 831
Bellamy, L. J. 1960, The Infrared Spectra of Complex Molecules (London: Methuen)
Boogert, A., Schutte, W., Helmich, F., & Tielens, A. G. G. M. 1995, in preparation
Butchart, I., McFadzean, A. D., Whittet, D. C. B., Geballe, T. R., & Greenberg, J. M. 1986, A&A, 154, L5
Cohen, M., Witteborn, F. C., Carbon, D. F., Auguson, G., Wooden, D., Bregman, J., & Goorvitch, D. 1992, AJ, 104, 2045
Cohen, M., Witteborn, F. C., Walker, R., Bregman, J., & Wooden, D. 1995, AJ, 110, 275
de Vries, R. C. 1987, Ann. Rev. Mater. Sci., 17, 161
d'Hendecourt, L. B., & Allamandola, L. J. 1986, A&AS, 64, 453
d'Hendecourt, L. B., Allamandola, L. J., Grim, R. J. A., & Greenberg, J. M. 1986, A&A, 158, 119
Draine, B. T. 1984, ApJ, 277, L71
———. 1989, in Interstellar Dust, ed. L. J. Allamandola & A. G. G. M. Tielens (Dordrecht: Kluwer), 313
Draine, B. T., & Lee, H. M. 1984, ApJ, 285, 89
Duley, W. W. 1993, in Dust and Chemistry in Astronomy, ed. T. J. Millar & D. A. Williams (Bristol: IOP), 71
Duley, W. W., & Williams, D. A. 1988, MNRAS, 230, 1P
Ehrenfreund, P., Robert, F., d'Hendecourt, L., & Behar, F. 1991, A&A, 252, 712
Ferraro, J. R. 1982, The Sadtler Infrared Spectra Handbook of Minerals and Clays (Philadelphia: Sadtler Research Laboratories)
Furton, D. G., & Witt, A. N. 1992, ApJ, 386, 587
———. 1993, ApJ, 415, L51
Gezari, D. Y., Tresch-Fienberg, R., Fazio, G. G., Hoffmann, W. F., Gatley, I., Lamb, G., Shu, P., & McCreight, C. 1985, ApJ, 299, 1007
Gilra, D. P. 1973, in The Scientific Results from the Orbiting Astronomical Observatory *OAO-2*, ed. A. D. Code (NASA SP-310), 297
Greenberg, J. M. 1979, in Stars and Starsystems, ed. B. E. Westerlund (Dordrecht: Reidel), 173
Greenberg, J. M., & Chlewicki, G. 1984, ApJ, 272, 563
Greenberg, J. M., & Hong, S. S. 1974, IAU Symp. 60, Galactic Radio Astronomy, ed. F. J. Kerr & S. C. Simonson (Dordrecht: Reidel), 155
Gribov, L. A., & Smirnov, V. N. 1962, Soviet Phys.—Uspekhi, 4, 919
Hagen, W. 1982, Ph.D. thesis, Rijksuniv. Leiden

Hagen, W., Allamandola, L. J., & Greenberg, J. M. 1979, Ap&SS, 65, 215
Hagen, W., Tielens, A. G. G. M., & Greenberg, J. M. 1981, Chem. Phys., 56, 367
———. 1983, A&AS, 51, 389
Huss, G. R., Fahey, A. I., Gallino, R., & Wasserburg, G. J. 1994, ApJ, 430, L81
Hutcheon, I. D., Huss, G. R., Fahey, A. I., & Wasserburg, G. J. 1994, ApJ, 425, L97
Jenniskens, P., Baratta, G. A., Kouchi, A., de Groot, M. S., Greenberg, J. M., & Strazzulla, G. 1993, A&A, 273, 583
Jones, A. P., Duley, W. W., & Williams, D. A. 1990, QJRAS, 31, 567
Jones, T. J., Hyland, A. R., & Allen, D. A. 1983, MNRAS, 205, 187
Jones, A. P., Tielens, A. G. G. M., Hollenbach, D. J., & McKee, C. F. 1994, ApJ, 433, 797
Lewis, R. S., Anders, E., & Draine, B. T. 1989, Nature, 339, 117
Lewis, R. S., Tang, M., Wacker, J. F., Anders, E., & Steel, E. 1987, Nature, 326, 160
Mathis, J. S. 1979, ApJ, 232, 747
———. 1995, in Polarimetry of the Interstellar Medium, ed. W. G. Roberge & D. C. B. Whittet (San Francisco: ASP), in press
Mathis, J. S., Rumpl, W., & Nordsieck, K. H. 1977, ApJ, 217, 425
McFadzean, A. D., Whittet, D. C. B., Longmore, A. J., Bode, M. F., & Adamson, A. J. 1989, MNRAS, 241, 873
McKee, C. F. 1989, in Interstellar Dust, ed. L. J. Allamandola & A. G. G. M. Tielens (Dordrecht: Kluwer), 431
Milligan, D. E., & Jacox, M. E. 1971, J. Chem. Phys., 54, 927
Onaka, T., de Jong, T., & Willems, F. P. 1989, A&A, 218, 169
Pendleton, Y. J., Sandford, S. A., Allamandola, L. J., Tielens, A. G. G. M., & Sellgren, K. 1994, ApJ, 437, 683
Purcell, E. M. 1969, ApJ, 158, 433
Rieke, G. H., & Low, F. J. 1973, ApJ, 184, 415
Rieke, G. H., Rieke, M. J., & Paul, A. E. 1989, ApJ, 336, 752
Rieke, G. H., Telesco, C. M., & Harper, D. A. 1978, ApJ, 220, 556
Robertson, J. 1986, Adv. Phys., 35, 317
Roche, P. F., & Aitken, D. K. 1984, MNRAS, 208, 481
———. 1985, MNRAS, 215, 425
Sandford, S. A., Allamandola, L. J., Tielens, A. G. G. M., Sellgren, K., Tapia, M., & Pendleton, Y. 1991, ApJ, 371, 607
Schmidt, G. D., Cohen, M., & Margon, B. 1980, ApJ, 239, L33
Schutte, W. 1988, PhD, thesis, Rijksuniv. Leiden
Schutte, W., & Greenberg, J. M. 1988, in Dust in the Universe, ed. M. E. Bailey & D. A. Williams (Cambridge: Cambridge Univ. Press), 403
Seab, C. G. 1987, in Interstellar Processes, ed. D. Hollenbach & H. Thronson (Dordrecht: Kluwer), 491
Sellgren, K., Brooke, T. Y., Smith, R. G., & Geballe, T. R. 1995, ApJ, 449, L69
Smith, R. G., Sellgren, K., & Tokunaga, A. T. 1989, ApJ, 344, 413
Spitzer, L. 1978, Physical Processes in the Interstellar Medium (New York: Wiley)
Tielens, A. G. G. M. 1989, in Interstellar Dust, ed. L. J. Allamandola & A. G. G. M. Tielens (Dordrecht: Kluwer), 239
———. 1990, in Submillimeter and Millimeter Astronomy, ed. G. Watt & A. Webster (Dordrecht: Kluwer), 13
Tielens, A. G. G. M., & Allamandola, L. J. 1987a, in Physical Processes in Interstellar Clouds, ed. G. Morfill & M. Scholer (Dordrecht: Kluwer), 333
———. 1987b, in Interstellar Processes, ed. D. Hollenbach & H. Thronson (Dordrecht: Kluwer), 397
Tielens, A. G. G. M., Allamandola, L. J., & Sandford, S. A. 1991, in Solid State Astrophysics, ed. E. Bussoletti & G. Strazulla (Amsterdam: North Holland), 29
Tielens, A. G. G. M., McKee, C. F., Seab, C. G., & Hollenbach, D. J. 1994, ApJ, 431, 321
van Thiel, M., Becker, E. D., & Pimentel, G. C. 1957, J. Chem. Phys., 27, 486
Vardya, M. S., de Jong, T., & Willems, F. J. 1986, ApJ, 304, L29
Wada, S., Sakata, A., & Tokunaga, A. T. 1991, ApJ, 375, L17
Wexler, A. S. 1967, Appl. Spectrosc. Rev., 1, 29
Whittet, D. C. B., Duley, W. W., & Martin, P. 1990, MNRAS, 244, 427
Willner, S. P., Russell, R. W., Puetter, R. C., Soifer, B. T., & Harvey, P. M. 1979, ApJ, 229, L65
Witt, A. N., & Boroson, T. A. 1990, ApJ, 355, 182
Witt, A. N., & Furton, D. G. 1995, in The Diffuse Interstellar Bands, ed. A. G. G. M. Tielens & T. P. Snow (Dordrecht: Kluwer), 149
Witt, A. N., & Schild, R. E. 1986, ApJS, 62, 839
Witteborn, F. C., & Bregman, J. 1984, Proc. SPIE, 509, 123
Witteborn, F. C., Cohen, M., Bregman, J., Heere, K. R., Greene, T. P., & Wooden, D. H. 1995, in Airborne Astronomy Symposium on the Galactic Ecosystem: From Gas to Stars to Dust, ed. M. R. Haas, J. Davidson, & E. Erickson (San Francisco), 573
Yorke, H. 1996, in The Role of Dust in the Formation of Stars, ed. H. U. Käufl & R. Siebenmorgen (Berlin: Springer), in press
Zinner, E., Amari, S., Wopenka, B., & Lewis, R. S. 1995, Meteoritics, 30, 209